



ELSEVIER



Available online at www.sciencedirect.com

ScienceDirect

Energy Reports 8 (2022) 361–368



www.elsevier.com/locate/egyr

2021 8th International Conference on Power and Energy Systems Engineering (CPESE 2021),
10–12 September 2021, Fukuoka, Japan

Electric field analysis of 66 kV and 110 kV SiR insulators under combined AC–DC voltages

Mehmet Murat Ispirli^{a,b,*}, Bülent Oral^a, Özcan Kalenderli^b

^a Department of Electrical-Electronics Engineering, Marmara University, 34722 Kadiköy, Istanbul, Turkey

^b Department of Electrical Engineering, Istanbul Technical University, 34469 Maslak, Istanbul, Turkey

Received 25 October 2021; accepted 8 November 2021

Available online 27 November 2021

Abstract

Insulators are the most crucial part of power systems. The insulation performance of insulators is vital for the sustainability of power systems. Recently, silicone rubber (SiR) insulators are used frequently in all sections of the power systems. In this paper, a SiR insulator currently used in power transmission systems has been analyzed under combined AC–DC voltage using the finite element method. In the analysis, positive and negative DC voltages in different amplitude ratios were superimposed over the phase-earth operating voltage of the insulator. Analyses in the study were made in time-dependent. Only DC voltage was applied to the insulator for the first 60 s, AC + DC voltage was applied between 60 to 120 s. Thus, the electric field behavior of the SiR insulator under combined AC–DC voltage has been obtained. The change of electric field based on positive and negative DC components was investigated. As a result of the study, the effect of the polarity of the DC component in the combined voltage was observed. As a result, effect of the polarity of the DC component in the combined voltage on the maximum electric field intensity was observed.

© 2021 The Author(s). Published by Elsevier Ltd. This is an open access article under the CC BY-NC-ND license (<http://creativecommons.org/licenses/by-nc-nd/4.0/>).

Peer-review under responsibility of the scientific committee of the 2021 8th International Conference on Power and Energy Systems Engineering, CPESE, 2021.

Keywords: Composite voltage; Combined voltage; Finite element analysis; SiR insulators

1. Introduction

Insulators are essential components of power transmission and distribution systems. The materials used in insulator production can be selected according to the place of use and working conditions of the insulator. They can be glass, ceramic, and silicone–rubber (SiR) [1]. Recently, SiR insulators are widely used in practice because of their advantages. The most benefits of SiR insulators are good dielectric performance, lightweight, easy transportation, anti-pollution properties and hydrophobic nature, easy production, less cost, and better electrical resistance [2].

* Corresponding author at: Department of Electrical-Electronics Engineering, Marmara University, 34722 Kadiköy, Istanbul, Turkey.
E-mail address: mispirl@marmara.edu.tr (M.M. Ispirli).

<https://doi.org/10.1016/j.egyr.2021.11.149>

2352-4847/© 2021 The Author(s). Published by Elsevier Ltd. This is an open access article under the CC BY-NC-ND license (<http://creativecommons.org/licenses/by-nc-nd/4.0/>).

Peer-review under responsibility of the scientific committee of the 2021 8th International Conference on Power and Energy Systems Engineering, CPESE, 2021.

One of the most important criteria in insulator selection is the electric field distribution around the insulator. The geometry and dimensions of insulation, ingredients of the material are affected the electric field distribution on its surface. Electric field distribution determines the discharge path of insulators [3].

The dielectric tests are carried out separately for AC, DC, or impulse voltages in many standards used for testing insulation materials. As a result of these experiments, the electric field behavior of the insulation material under only DC, only AC, and only impulse voltage is obtained. However, in real application, insulation materials are not forced by a single type voltage. They are strained by combined voltages such as AC + lightning impulse, AC + DC, etc. After a switching operation or any fault, the transient pole voltage, contains a ripple which may last for a few cycles of power frequency. Such a voltage waveshape may be accepted as AC + DC composite waveform [4]. For this reason, testing the insulation materials under the combined voltages will increase the security and reliability level of the systems. The combined voltages are formed by the combination of two signals having different wave shapes [5]. In the literature, there are few studies for the investigation of discharge phenomena under the combined voltages [6–11]. There are many studies in the literature on the investigation of insulator electric field behavior using finite element method (FEM) under a single type voltage, such as only AC voltage [12–15]. In this study, unlike the literature, the electric field behavior of SiR insulators was analyzed under combined AC + DC voltages using FEM. For these analyses, time-dependent models were created.

In this paper, the electric field distribution of 66 kV and 110 kV SiR insulators was investigated under the combined AC + DC voltages by using the FEM. Analyses were made time-dependent during the 120 s. Firstly, the electric field distribution of insulators was computed for the 50 Hz AC voltage. Later, DC voltage was applied for the first 60 s, and 50 Hz AC voltage was superimposed on DC voltage after 60 s. The electric field analyses of insulators were performed under this combined voltage.

2. Material and method

In this study, the electric field distribution of SiR insulators was obtained by using a package program based on FEM. The finite element method is a numerical method that is frequently used in the solution of engineering problems. This method is commonly used to obtain the electric field distribution of an insulating material and to model the insulation performance in high voltage technique applications [15–18].

The following steps are applied when conducting electric field analysis with FEM:

1. First, the geometric figure of the problem is drawn, and on the figure drawn, the materials of the problem are defined.
2. The boundary conditions of the problem are appointed.
3. Solution region containing the geometric figure of the problem is divided into triangular finite elements, and the basic equations for these elements are defined according to boundary conditions.
4. Finally, the set of mathematical equations obtained from all these definitions is solved by the package program.

In the simulation studies, 66 kV and 110 kV SiR overhead line insulators were considered. The 2D CAD drawing of axial section of these insulators according to symmetry axis was shown in Fig. 1. The lengths of the insulators are 76.2 cm and 114 cm, respectively. The 66 kV insulator consists of 14 sheds with a 62.7 mm radius, while the 110 kV insulator consists of 20 sheds with a 64.8 mm radius.

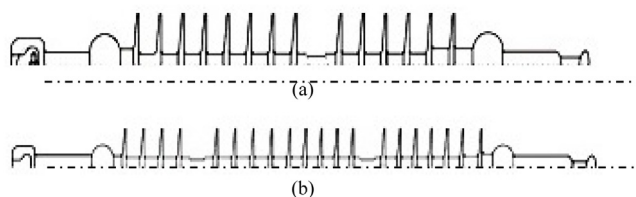


Fig. 1. The 2D drawing of SiR insulator as axial symmetry (a) 66 kV (b) 110 kV.

While the package program we have used allows making drawings within itself, it also provides the opportunity to import 2D or 3D CAD files designed by another software. Due to its semi-analytical approach, determining special equations and combining these equations by the program provides excellent advantages in terms of usage [19].

With its time-dependent study feature, this program can analyze the time domain. This feature allows modeling of electric field behavior of materials under combined voltages.

In this study, to define the closed solution region, the air environment with a radius of 100 cm has been drawn around the 66 kV and 110 kV insulators shown in Fig. 1. The geometry of the model formed in the package program is shown in Fig. 2. The defined materials and their properties in the models are shown in Table 1.

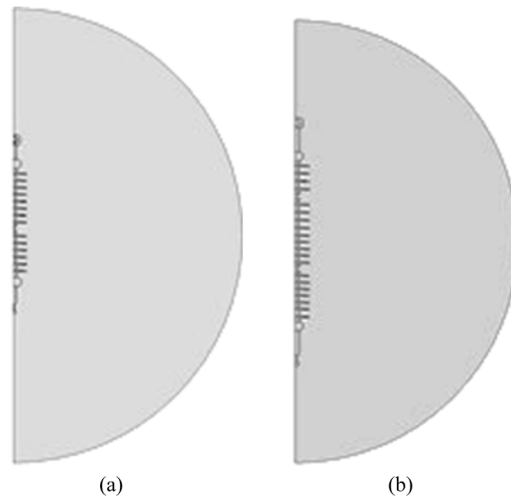


Fig. 2. The 2D model of SiR insulator as axial symmetry: (a) 66 kV; (b) 110 kV.

Table 1. The defined materials and their properties in the models.

Object	Materials	Relative permittivity	Conductivity (S/m)
Insulation medium	Air	1	10^{-15}
Insulator	Silicone-rubber	3	10^{-13}
Metal fittings	Soft iron	1	1.12×10^7

In the problem figure drawn, the top end potential of the insulator is defined as ground, while the lower end of the insulator is applied as 50 Hz AC and combined AC–DC voltage. When defining combined AC–DC voltage, Eq. (1) was used. Where, while determining the DC component of the combined voltage, 1%, 3%, 5%, and 10% of U_p were taken, respectively.

$$V_s(t) = U_p \sin(\omega t) \pm 0.01 \cdot p \cdot U_p \tag{1}$$

In this equation;

$V_s(t)$: Superimposed voltage dependent on time

U_p : The peak value of the phase to neutral voltage of the insulator

p : Percent value

ω : Angular frequency, $\omega = 2\pi f$

t : Time (s)

After the geometry of the model, materials, and boundary conditions are defined, the model was divided into finite elements. The defined equations in this model are as follows;

$$\nabla \cdot J = -\frac{\partial \rho}{\partial t} \tag{2}$$

$$E = -\nabla V \tag{3}$$

$$J = \sigma E + \frac{\partial D}{\partial t} + J_e \tag{4}$$

Where;

- ∇ : Differential operator (nabla operator)
- J : Current density
- D : Electric displacement
- ρ : Charge density
- E : Electric field intensity
- V : Electric potential
- J_e : External current density
- t : Time
- σ : Electrical conductivity (S/m)

3. Results

3.1. Electric field analysis of 66 kV SiR insulator under combined AC + DC voltages

Firstly, in this part of the study, the 66 kV SiR insulator was analyzed only under AC voltage with FEM. The value of the applied AC voltage is the nominal phase-to-ground voltage of the insulator. Later, the insulator has been analyzed under combined AC + DC voltage with FEM, and the electric field distributions have been obtained. In these analyses, the values of DC voltage are 1%, 3%, 5%, and 10% of the peak of AC voltage. These voltages were superimposed over the AC voltage as positive and negative. After only DC voltage was applied to the insulator during the first 60 s, AC + DC voltage was applied between 60 to 120 s. In the analyses, the maximum and average electric field intensities were calculated from the first three sheds on the HV side and the first three sheds on the LV. Later, the maximum electric field intensity in the model was found by means of the package program. These calculated values were compared with the electric field values found for only AC voltage. The electric field behavior of 66 kV SiR insulator under the combined AC + DC voltage was evaluated with these three calculated parameters.

Compared to under only AC voltage, the maximum electric fields along the first three sheds on the HV side and the first three sheds on the LV side under combined AC–DC voltage with different DC ratios were shown in Fig. 3(a). Although the peak value of voltage increased under AC + DC combined voltage, the maximum electric field value for the other five sheds except for the first shed on the HV side decreased compared to only AC. In the first shed on the HV side, it is almost unchanged. Although the peak value of voltage increased under 5% –DC + AC combined voltage, the maximum electric field value for all six sheds decreased compared to AC. Here, the maximum reduction in the electric field intensity was seen at the first shed on the HV side. In the first shed on the HV side, the electric field intensity increased significantly after 5% –DC and 1% +DC voltage.

Compared to under only AC voltage, the average electric field intensities along the first three sheds on the HV side and the first three sheds on the LV side under combined AC + DC voltage with different DC ratios were shown in Fig. 3(b). For 1% ± DC voltage, the increase in the average electric field value on the 3rd sheds on the HV and LV side was more than 1%, while it increases on the other four sheds was less than 1%. For 10% ± DC voltage, the average electric field value on the 3rd sheds on the HV and LV side increased significantly. In the case that both positive and negative DC voltages are superimposed, although the peak value of combined voltage increases by 10%, the average electric field strength increased between 16% and 17.5%.

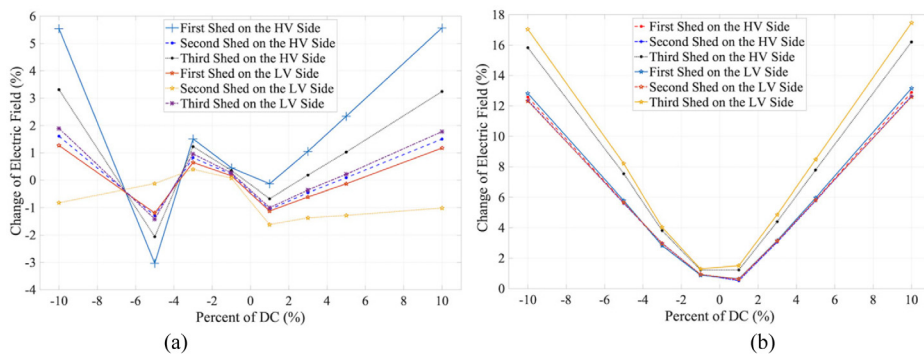


Fig. 3. The change of 66 kV SiR insulator under combined AC + DC voltage compared to only AC (a) maximum electric field (b) average electric field.

The change of maximum electric field intensity compared to under only AC voltage and maximum electric field on the insulator surface under combined AC + DC voltage with different DC ratios were shown in Fig. 4. The maximum electric field and electric field distribution on 66 kV SiR insulator surface were shown in Fig. 5 for

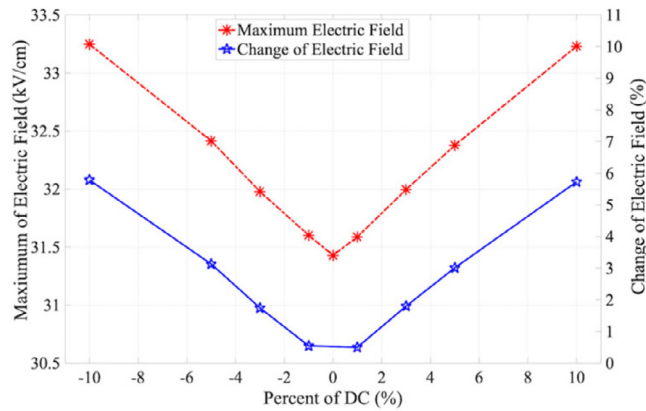


Fig. 4. The maximum electric field on 66 kV SiR insulator surface and the change of maximum electric field under combined AC + DC voltage compared to only AC.

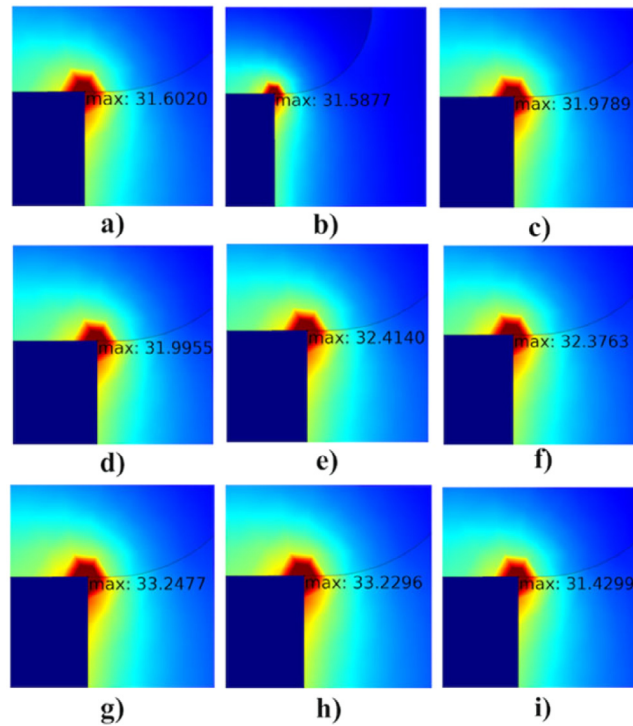


Fig. 5. The maximum electric field and electric field distribution on 66 kV SiR insulator surface: (a) AC - 1%DC; (b) AC + 1%DC; (c) AC - 3%DC; (d) AC + 3%DC; (e) AC - 5%DC; (f) AC + 5%DC; (g) AC - 10%DC; (h) AC + 10%DC; (i) only AC.

different DC ratios. In all cases, the rate of increase of the maximum electric field intensity was less than the rate of increase of the peak value of the combined AC + DC voltage. For all ratios except 3% DC, the maximum electric field intensity of the superimposed negative DC voltage was greater than the maximum electric field intensity of the superimposed positive DC voltage. In all cases, the maximum electric field occurred in the same area of the insulator.

3.2. Electric field analysis of 110 kV SiR insulator under combined AC + DC voltages

In this part of the study, as in the first part, the 110 kV SiR insulator was first analyzed under AC only voltage. The value of the applied AC voltage is the nominal phase-to-ground voltage of the insulator. Then, as in the first part of the study, only \pm DC voltage was applied at different rates during the first 60 s, and the AC voltage was superposed between 60 to 120 s. In these analyses, the DC voltage values are 1%, 3%, 5%, and 10% of the peak of AC voltage. Here, as in the first part, evaluations are done by calculating the maximum and average electric field values along first three sheds on the HV side and the first three sheds on the LV side.

Compared to under only AC voltage, the maximum electric fields along the first three sheds on the HV side and the first three sheds on the LV side under combined AC–DC voltage with different DC ratios were shown in Fig. 6(a). Although the peak value of the voltage increased under 1% DC + AC combined voltage, the maximum electric field intensity has decreased in all sheds. Although the peak value of the voltage increased under 3% DC + AC combined voltage, while the maximum electric field intensity in all sheds on the LV side decreased, it in all sheds on the HV side increased. However, although the increase in the voltage value is 3%, the increase in the maximum electric field intensity is less than 1%. The maximum electric field in all sheds on the LV side under 5% –DC + AC combined voltages is lower than the maximum electric field in all sheds on the LV side under 3% –DC + AC combined voltages. The maximum electric field in the first two sheds on the LV side under 5% –DC + AC combined voltages is equal to under only AC voltages. For all rates except 5% DC, the maximum electric field intensity formed by negative DC voltage is greater than the positive DC voltage.

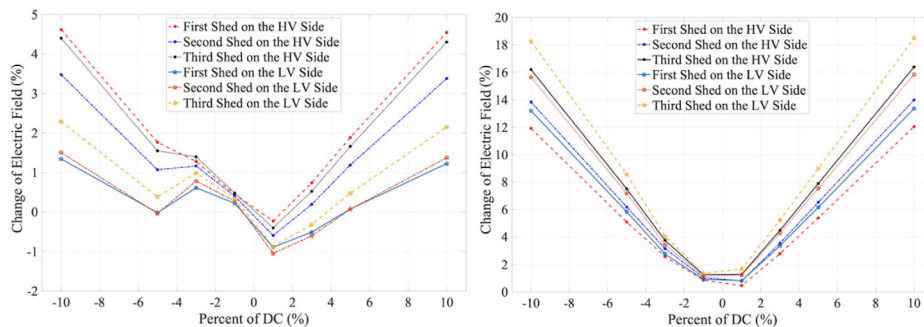


Fig. 6. The change of 110 kV SiR insulator under combined AC + DC voltage compared to only AC (a) maximum electric field (b) average electric field.

Compared to under only AC voltage, the average electric fields along the first three sheds on the HV side and the first three sheds on the LV side under combined AC–DC voltage with different DC ratios were shown in Fig. 6(b). In the analysis for 1%, 3%, and 5% positive and negative DC, the average electric field in the first and second sheds on the HV and LV side increased approximately equal to the percentage of DC. However, the average electric field in the third sheds on HV and LV side is greater than the percentage of DC for 1%, 3%, and 5% positive and negative DC.

In the analysis for positive and negative 10% DC, the increase of average electric field in all sheds on the HV and LV side is greater than 10%. In particular, the increase in the 3rd sheds on the HV and LV sides is much greater. They are almost 16% and 18%, respectively. In the analysis for 1%, 3%, and 5% DC, the average electric field in the positive DC is greater than negative DC for all sheds on the HV and LV side. But it is unstable for 1% DC.

The change of maximum electric field compared to under only AC voltage and maximum electric field on the insulator surface under combined AC–DC voltage with different DC ratios were shown in Fig. 7. The maximum electric field and electric field distribution on 110 kV SiR insulator surface were shown in Fig. 8 for different DC ratios. In all cases, the rate of increase of the maximum electric field was less than the rate of increase of the peak value of the combined AC–DC voltage. For all ratios except 10% DC, the maximum electric field intensity of the superimposed positive DC voltage was greater than the maximum electric field intensity of the superimposed negative DC voltage. In all cases, the maximum electric field occurred in the same area of the insulator.

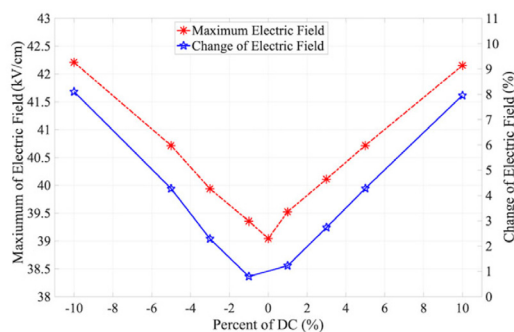


Fig. 7. The maximum electric field on 110 kV SiR insulator surface and the change of maximum electric field under combined AC–DC voltage compared to only AC.

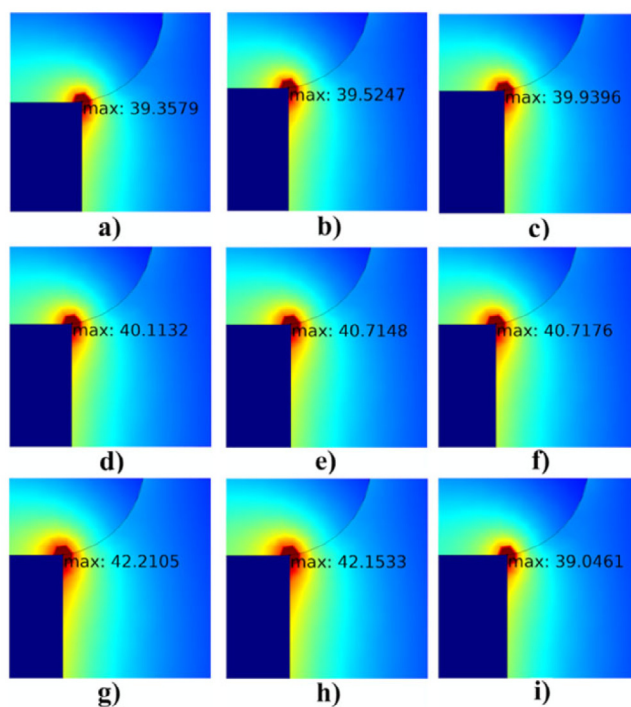


Fig. 8. The maximum electric field and electric field distribution on 110 kV SiR insulator surface: (a) AC - 1%DC; (b) AC + 1%DC; (c) AC - 3%DC; (d) AC + 3%DC; (e) AC - 5%DC; (f) AC + 5%DC; (g) AC - 10%DC; (h) AC + 10%DC; (i) only AC.

4. Conclusion

In this study, 66 kV and 110 kV SiR insulators have been analyzed by using finite element method under superimposed voltage containing different proportions of positive and negative DC components. As a result of these analyses;

- In the analyses in 66 kV SiR insulator, 5% -DC and 1% +DC superimposed over the AC are the critical point for maximum electric field on the sheds of the insulator. Although the peak value of combined voltage increased, the maximum electric field on the sheds of the insulator was decreased significantly in these points.
- In 66 kV SiR insulator, the negative DC has been more effective more than positive DC in terms of the change of maximum electric field on the insulator surface. Whereas, in the 110 kV SiR, the positive DC has been more effective than the negative DC in terms of the change of maximum electric field on the insulator surface.

- The average electric field in all sheds of 66 kV SiR and 110 kV insulator increased much more than 10% for both positive and negative DC voltages, although the peak value of combined voltage increases by 10%.
- In the analyses in 110 kV SiR insulator, 1% +DC superimposed over the AC is the critical point for maximum electric field on all sheds of the insulator. After this point, it increased significantly for superimposed +DC voltage.

The maximum electric field strength is generally important in whether to initiate a discharge event or not. It is known that a discharge event occurs when the maximum electric field strength is equal to or higher than the dielectric strength. This study has seen the effect of the polarity of the DC component in combined voltage. The maximum electric field intensity is especially significantly affected by the polarity of the DC component in combined voltage.

Declaration of competing interest

The authors declare that they have no known competing financial interests or personal relationships that could have appeared to influence the work reported in this paper.

Acknowledgment

The authors would like to thank Marmara University, Turkey Scientific Research Projects Commission for its support in the form of a Grant (FEN-A-130219-0031).

References

- [1] Malik NH, Al-Arainy AA, Qureshi MI. Electrical insulation in power systems. Marcel Dekker; 1998. <http://dx.doi.org/10.1109/MEI.1998.689277>.
- [2] El-Hag AH. Leakage current characterization for estimating the conditions of non-ceramic insulators surfaces. *Electr Power Syst Res* 2017;77:379–84. <http://dx.doi.org/10.1016/j.epsr.2006.03.018>.
- [3] Zhang B, Han S, He J, Zeng R, Zhu P. Numerical analysis of electric-field distribution around composite insulator and head of transmission tower. *IEEE Trans Power Deliv* 2006;21(2):959–65. <http://dx.doi.org/10.1109/TPWRD.2005.859293>.
- [4] Grzybowski S, Kuffel E. Electrical breakdown strength of polypropylene film oil-immersed under combined AC-DC voltage. In: Conference on electrical insulation & dielectric phenomena - annual report 1986. 1986, p. 516–21. <http://dx.doi.org/10.1109/CEIDP.1986.7726493>.
- [5] Kalenderli Ö, Önal E. Design of composite high voltage generation circuits. In: Conference on electrical-electronics and biomedical engineering. Bursa, Turkey. 2016. p. 1–3.
- [6] Sha Y, Zhou Y, Zhang L, Huang M, Jin F. Measurement and simulation of partial discharge in oil-paper insulation under the combined AC–DC voltage. *J Electrostat* 2013;71(3):540–6. <http://dx.doi.org/10.1016/j.elstat.2012.11.013>.
- [7] Li S, Si W, Li Q. Partition and recognition of partial discharge development stages in oil-pressboard insulation with needle-plate electrodes under combined AC-DC voltage stress. *IEEE Trans Dielectr Electr Insul* 2017;24(3):1781–93. <http://dx.doi.org/10.1109/TDEI.2017.006361>.
- [8] Liu M, Liu Y, Li Y, Zheng P, Rui H. Growth and partial discharge characteristics of electrical tree in XLPE under AC-DC composite voltage. *IEEE Trans Dielectr Electr Insul* 2017;24(4):2282–90. <http://dx.doi.org/10.1109/TDEI.2017.006537>.
- [9] Seifert F, Porizka I, Leu C. Charge accumulation at high DC voltage and superimposed medium frequency AC voltage. In: IEEE 3rd international conference on dielectrics. Valencia, Spain; 2020, p. 333–7. <http://dx.doi.org/10.1109/ICD46958.2020.9341963>.
- [10] Du BX, Yang ZR, Li ZL, Li J. Temperature-dependent charge property of silicone rubber/SiC composites under lightning impulse superimposed DC voltage. *IEEE Trans Dielectr Electr Insul* 2019;26(3):810–7. <http://dx.doi.org/10.1109/TDEI.2018.007771>.
- [11] Xiong Q, et al. Flashover performance of silicon rubber under combined AC-DC voltage and its improving method. *IEEE Trans Dielectr Electr Insul* 2018;25(1):272–80. <http://dx.doi.org/10.1109/TDEI.2018.006677>.
- [12] Stefanini D, Seifert JM, Clemens M, Weida D. Three dimensional FEM electrical field calculations for EHV composite insulator strings. In: IEEE international power modulator and high voltage conference. 2010, p. 238–42. <http://dx.doi.org/10.1109/IPMHVC.2010.5958337>.
- [13] M'hamdi B, Tegar M, Mekhaldi A. Optimal design of corona ring on HV composite insulator using PSO approach with dynamic population size. *IEEE Trans Dielectr Electr Insul* 2016;23(2):1048–57. <http://dx.doi.org/10.1109/TDEI.2015.005383>.
- [14] Nia MS, Altmanian M, Shamsi P, M. Ferdowsi M. Comprehensive analysis for electric field and potential for polymeric and ceramic insulators. *Am J Electr Electron Eng* 2020;8(1):26–34. <http://dx.doi.org/10.12691/ajeee-8-1-4>.
- [15] Uckol HI, Karaca B, S. Ilhan S. DC and AC electric field analysis and experimental verification of a silicone rubber insulator. *Electr Eng* 2020;102:503–14. <http://dx.doi.org/10.1007/s00202-020-00954-3>.
- [16] Ispirli MM, Yilmaz AE, Kalenderli Ö. Investigation of tracking phenomenon in cable joints as 3D with finite element method. *Electr Eng* 2018;100(4):2193–203. <http://dx.doi.org/10.1007/s00202-018-0696-6>.
- [17] Aouabed F, Bayadi A, Rahmani AE, Boudissa R. Finite element modelling of electric field and voltage distribution on a silicone insulating surface covered with water droplets. *IEEE Trans Dielectr Electr Insul* 2018;25(2):413–20. <http://dx.doi.org/10.1109/TDEI.2017.006568>.
- [18] Talaat M, El-Zein A, Amin M. Electric field simulation for uniform and FGM cone type spacer with adhering spherical conducting particle in GIS. *IEEE Trans Dielectr Electr Insul* 2018;25(1):339–51. <http://dx.doi.org/10.1109/TDEI.2018.006980>.
- [19] Zimmerman WBJ. *Multiphysics modeling with finite element methods*, vol. 18. World Scientific Publishing Company; 2006.